Antineoplastic Agents. 579. Synthesis and Cancer Cell Growth Evaluation of *E*-Stilstatin 3: A Resveratrol Structural Modification[⊥]

George R. Pettit,* Noeleen Melody, Andrew Thornhill, John C. Knight, Thomas L. Groy, and Cherry L. Herald

Cancer Research Institute and Department of Chemistry and Biochemistry, Arizona State University, P.O. Box 871604, Tempe, Arizona 85287-1604

Received April 9, 2009

As an extension of our earlier structure/activity investigation of resveratrol (**1a**) cancer cell growth inhibitory activity compared to the structurally related stilbene combretastatin series (e.g., **2a**), an efficient synthesis of *E*-stilstatin 3 (**3a**) and its phosphate prodrug **3b** was completed. The *trans*-stilbene **3a** was obtained using a convergent synthesis employing a Wittig reaction with phosphonium bromide **9** as the key reaction step. Deprotection of the *Z*-silyl ether **13** gave *E*-stilstatin 3 (**3a**) as the exclusive product. The structure and stereochemistry of **3a** was confirmed by X-ray crystal structure determination.

The therapeutic potential of the *E*-stilbene resveratrol (**1a**),[2a] first isolated from roots of *Vertarum grandiflorum* (white hellebore) in 1940, covers a wide range of diseases as noted in recent reviews.[2b,c] Stilbene **1a** has been reported to be an inhibitor of carcinogenesis at multiple stages via its ability to inhibit cyclooxygenase[3a,b] and is an anticancer agent with a role in antiangiogenesis[2a,4] and in the upregulation of phase II enzymes, which are involved in detoxifying harmful metabolites and are therefore an indication of chemopreventive activity.[2a,5] More recently both in vitro and in vivo studies showed that stilbene **1a** induces cell cycle arrest and apoptosis in tumor cells.[6] The cardioprotective effects of resveratrol have been found to include prevention of platelet aggregation in vitro,[7] promotion of vasorelaxation,[8,9] prevention of LDL oxidation,[10] and reduced formation of atherosclerotic plaques and restoration of flow-mediated dilation in rabbits fed on a high-cholesterol diet.[11] Resveratrol's (**1a**) inhibition of cyclooxygenase enzymes[3] led to the discovery that, along with suppression of the apoptotic neuronal cell death initiated by neuroinflammation typical of Parkinson's disease[12a] as well as other inflammatory responses,[12b] specific immune responses were enhanced.[13] Resveratrol has been suggested to inhibit tissue death due to oxygen starvation during a heart attack or stroke.[14a,b] Very importantly, resveratrol's effects on longevity have been of increasing interest.[2c,15] In concert with these observations, stilbene **1a** and the related *Z*-stilbene combretastatin A-4 (**2a**) have been shown to improve fasting blood glucose levels and insulin resistance as summarized below.

An investigation of resveratrol metabolism in humans by Walle[16] revealed that **1a** was metabolized extensively in the body and that the bulk of an intravenous initial dose was rapidly converted (~30 min) to sulfate esters and other derivatives. Furthermore, when methylated analogue **1b** was investigated, it was found to be more active than the natural product in the majority of bioassays.[17] Such evidence raised the possibility that one (or more) of its many metabolites is the biologically active agent, rather than resveratrol itself, and has led to a number of investigations focused on the synthesis of new structural modifications of resveratrol (**1a**),[12b,18] including our earlier synthesis and biological study of sodium resverastatin phosphate prodrug[19j] and stilstatins 1 and 2.[1]

For over 30 years, we have been exploring the chemistry and the anticancer and other important biological properties of the combretastatins that we isolated from the South African bush willow

Scheme 1[a]
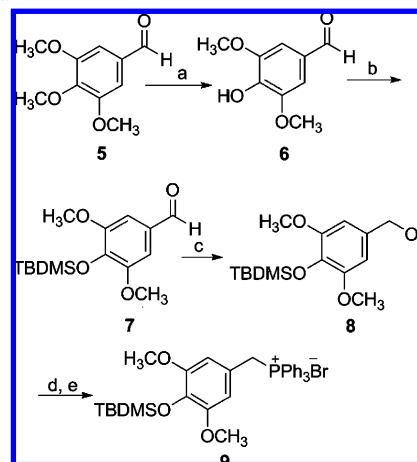
[a] Reagents and conditions: (a) piperidine/water, reflux, 48 h; (b) DIPEA, DMF, TBDMSCl, rt, 18 h; (c) NaBH₄, CH₃CH₂OH, 0 °C, rt, 2 h; (d) DCM, PBr₃, 0 °C, rt, 2 h; (e) toluene, PPh₃, rt, 24 h.

Combretum caffrum.[19] Among the combretastatins, the A-4 (**2a**, CA4)[19a] has received major attention owing to its strong inhibition of tubulin polymerization and selective targeting of tumor vascular systems (cancer vascular disrupting), which cuts off the tumor blood flow, leading to hemorrhagic necrosis as well as cancer antiangiogenesis.[20] After 10 years of advancing through phase I and II clinical trials, the prodrug sodium combretastatin A-4 phosphate (**2b**, CA4P) has now entered phase III human cancer clinical trials. In addition, CA4P has advanced to phase II human clinical trials against both myopic and wet macular degeneration (a leading cause of blindness). Current results from the clinical trials have been very encouraging and have stimulated a large number of important SAR[20a–c] and broad-spectrum biological/medical studies.[20a–c,21,22]

Among the latter investigations are the recent reports that CA4P strongly inhibits gastric tumor metastases by attenuating p-AKT expression (facilitates migration of cancer cells to distant tissue sites)[21] and that both CA4 (**2a**) and resveratrol (**1a**) activate AMPK (and downregulate gluconeogenic enzyme mRNA levels) in the liver, which improved the fasting blood glucose levels in diabetic db/db mice.[22] The AMPK studies with CA4 also showed, as with **1a**, that it activates PPAR transcriptional activity, which improved the glucose tolerance in the diabetic mice.[22] Overall these results, with AMPK serving as a useful therapeutic target for controlling type 2 diabetes and obesity, suggest another very important avenue for future resveratrol (**1a**) and CA4 (and CA4P) new drug research.[22]
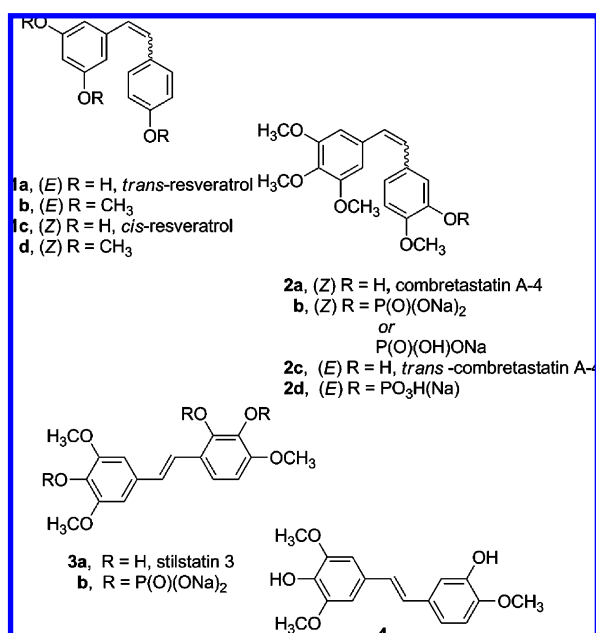
Scheme 2[a]
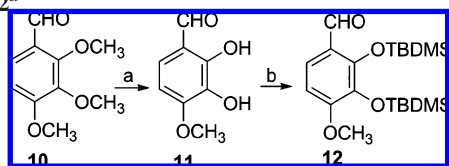
[a] Reagents and conditions: (a) DCM, BCl₃, 2 h, rt, BCl₃, rt, 24 h; (b) DMF, DIPEA, rt, TBDMS-Cl.

Because of the ever-increasing biological relationships of certain combretastatins to resveratrol (**1a**), we have continued our structure/activity investigations[19g,j,23] and now report the synthesis of a new structural modification of **1a**, the polyhydroxylated *trans*-stilbene designated stilstatin 3 (**3a**), and its phosphate prodrug (**3b**). Stilstatin 3 was evaluated first as a cancer cell growth inhibitor, and the data were compared with those of the structurally similar **1a** and **1c**, methylated derivatives **1b** and **1d**, combretastatin A4 isomers and salts **2a**−**d**, and the structural modification **4**.

1a, (E) R = H, *trans*-resveratrol
b, (E) R = CH₃
1c, (Z) R = H, *cis*-resveratrol
d, (Z) R = CH₃

2a, (Z) R = H, combretastatin A-4
b, (Z) R = P(O)(ONa)₂
or
P(O)(OH)ONa
2c, (E) R = H, *trans*-combretastatin A-4
2d, (E) R = PO₃H(Na)

3a, R = H, stilstatin 3
b, R = P(O)(ONa)₂

Results and Discussion

The experimental procedures[19] developed for our prior syntheses of combretastatins[19i] were modified to give *E*-stilstatin 3. Scheme 1 outlines the synthesis of the necessary phosphonium bromide, where intermediates **6** and **7** were prepared by modifications of prior methods. Silyl ether **7** was reduced to alcohol **8** followed by bromination and phosphorylation to give bromide **9**, the A-ring precursor of **3a**. Synthesis of the B-ring counterpart was begun as follows (Scheme 2). Commercially available aldehyde **10** was selectively demethylated with BCl₃ as previously described[19i] to furnish diphenol **11**. Subsequent protection[19d] with TBDMS-Cl gave access to aldehyde **12** in very good overall yields. A Wittig reaction sequence (Scheme 3) employing phosphonium bromide **9** and aldehyde **12** led to stilbene **3a**.

Treatment of **9** with *n*-butyllithium at −15 °C afforded the ylide, and addition of aldehyde **12** gave the silyl ethers **13** and **14**. The *cis*/*Z*-isomer was isolated (by fractional crystallization from ethanol) from the reaction product in 65% yield as a colorless crystalline compound. Further separation of the reaction products (now rich in *trans*/*E*) by recrystallization from CH₃OH−CH₂Cl₂ gave the *E* silyl ether as needles in ~10% yield, confirmed by NMR spectroscopic analysis. A number of attempts at desilylation of *Z*-isomer **13** using tetrabutylammonium fluoride (TBAF) did not yield the *Z* product but instead *E*-stilstatin 3 (**3a**). We have encountered the

**Table 1.** Human Cancer Cell Growth Inhibition Results (GI₅₀, µg/mL)

	cell line					
structure	pancreas BXPC-3	breast MCF-7	CNS SF-268	lung-NSC NCI-H460	colon KM20L2	prostate DU-145
1a[19j]	3.3	3.9	4.1	3.6	13.1	3.5
1b[19j]	0.35		0.56	0.62		1.5
1c[19j]	15.5	14.8	5.0	13.2	22.0	10.2
1d[19j]	0.0034		0.0044	0.0028		0.0054
2a[19j]	0.39	>0.01		0.00060	0.34	0.00080
2c[19g]	3.9			0.038		0.037
3a	>10	5.5	>10	>10	>10	>10
3b	>10	>10	>10	>10	>10	>10
4[23]	5.0			4.9		6.3

geometrical instability of related *Z*-isomers previously. For example, the *Z*-isomer of stilbene **4**[23] could be isolated but evaded biological investigations owing to isomerization to the *E*-stilbene **4** over 1 day (room temperature). *E*-Stilstatin 3 (**3a**) recrystallized from benzene−chloroform, and following initial characterization the geometry and overall structure were confirmed by an X-ray crystal structure determination (Figure 1).

Photochemical isomerization[24] of **3a** was also investigated as a route to the *Z*-isomer, which was needed for biological comparison and evaluation. For the *E* → *Z* conversion, *Z*-stilstatin 3 (**3a**) in benzene was stirred with benzil and irradiated with a 254 nm UV lamp for 29 h. The products were separated by column chromatography to afford only unreacted *E*-isomer. Further attempts at photochemical isomerization of the *E*-isomer in acetonitrile with fluorenone as the sensitizer[25] were also unsuccessful. Ultraviolet irradiation was conducted using a standard laboratory UV lamp at 365 nm (and at >280 nm) and also using a medium-pressure UV lamp under an argon atmosphere (photochemical cabinet) with the exclusion of light for 4 h. In the latter experiments, the light pink solution of **3a** turned dark orange over time, but examination by NMR did not reveal the *Z*-isomer as a product in any of these experiments.

Next **3a** was phosphorylated with dibenzylphosphite in the presence of CCl₄[19j,26] to give triphosphate **15**. The phosphoric acid intermediate was obtained by deprotection of **15** with TMS-Br at rt and was isolated following extraction of the reaction mixture with water. The sodium prodrug was obtained when the aqueous fraction was concentrated to a small volume and eluted through a column containing Dowex 50X8-200 ion-exchange resin (sodium form). The UV-active fractions were combined and freeze-dried to yield a cream solid, which was reprecipitated from a solution of ethanol−water at 0 °C overnight to yield sodium phosphate **3b** as a colorless crystalline powder in quantitative yield.

Stilstatin **3a** and its phosphate prodrug (**3b**) were found to exhibit less cancer cell growth inhibitory activity than resveratrol (**1a**), resveratrol analogue **1b**, and *E*-stilbene **4** against a panel of human cancer cell lines. Stilstatin **3a** showed moderate cytotoxicity (GI₅₀ 5.5 µg/mL) against the breast MCF-7 cell line. A comparison of cancer cell line data for the resveratrol synthetic modifications **1b**,[19j] **4**,[23] and **3a** showed a decrease in activity with successive addition of hydroxyl groups to the B-ring of the *E*-stilbene system. Our previous studies have shown the *E*-isomer of combretastatin A-4[19g] (**2c**) to be in some cases 100 times less active in various cancer cell lines than the remarkably potent *cis*-isomer **2a**. These results are consistent with general observations to date that the *E*-stilbenes are less active as cancer cell growth inhibitors compared to their *Z*-counterparts. The *Z*-isomer of resveratrol (**1c**) was the exception to this general rule and showed slightly less activity than the *E*-isomer (**1a**). However the methylated *Z*-isomer (**1d**) proved to be more active than its *E*-isomer (**1b**). Future investigation of stilstatin **3a** and the other resveratrol structural modifications noted herein as sirtuin activators along with the combretastatin series may provide further SAR insights.

Scheme 3[a]
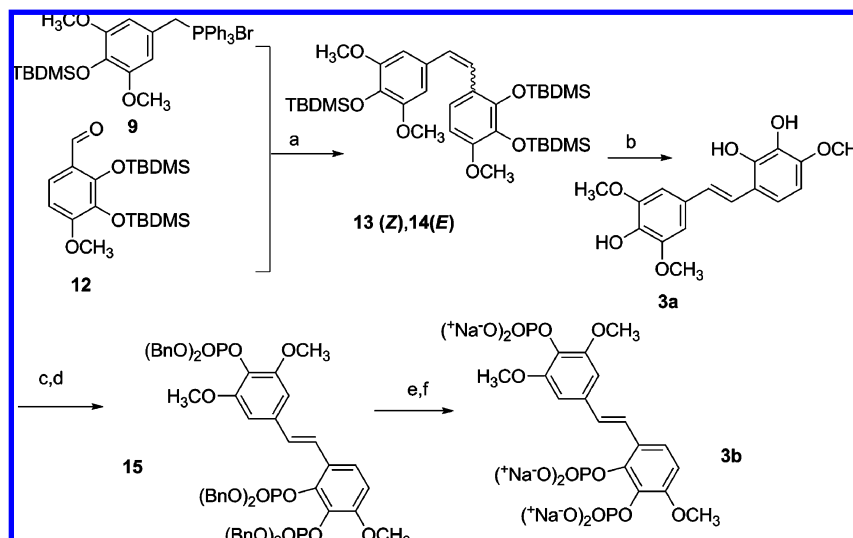
[a] Reagents and conditions: (a) *n*-BuLi, THF, −15 °C; (b) THF, −10 °C, TBAF (1 M in THF); (c) CCl₄, −10 °C, acetonitrile; (d) DIPEA, DMAP, dibenzyl phosphite; (e) TMS-Br, DCM, rt; (f) ion exchange, Dowex 50X8-200 (sodium form).
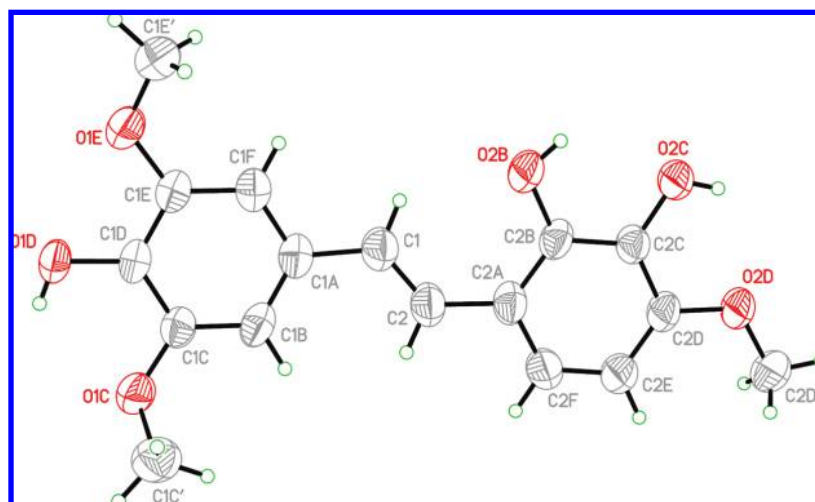

Figure 1. X-ray crystal structure of *E*-stilstatin 3 (**3a**).

Experimental Section

General Experimental Procedures. All solvents and reagents were obtained from Sigma-Aldrich (Milwaukee, WI) and Acros Organics (Fischer Scientific, Pittsburgh, PA). Ether refers to diethyl ether, and Ar refers to argon gas. All starting reagents were used as purchased unless otherwise stated. Reactions were monitored by TLC using Analtech silica gel GHLF uniplates visualized under long- and short-wave UV irradiation along with staining with phosphomolybdic acid/ heat, iodine, or KMnO₄. Where appropriate, the crude products were separated by flash column chromatography on silica gel (230−400 mesh ASTM) from E. Merck. The photochemical experiments were conducted with a standard laboratory UV lamp at 365 and 254 nm and with a medium-pressure mercury lamp at >280 nm in a photochemical cabinet under argon.

Melting points are uncorrected and were determined employing an electrothermal 9100 apparatus. The ^{1}H and ^{13}C NMR spectra were recorded employing Varian Gemini 300, Varian Unity 400, or Varian Unity 500 instruments using a deuterated solvent and were referenced to either TMS or the solvent. The reported figures are given as ppm. Phosphorus NMR was referenced against a standard of 85% H₃PO₄. HRMS data were recorded with a Jeol LCmate mass spectrometer and Jeol GCmate. Elemental analyses were determined by Galbraith Laboratories, Inc., Knoxville, TN.

4-Hydroxy-3,5-dimethoxybenzaldehyde (6). Preparation of compound **6** was repeated as originally described[27] from 3,4,5-trimethoxy-

benzaldehyde (**5**). Additional NMR and IR data are reported: 74% yield; mp 113−115 °C [lit.[27] mp 113−114 °C]; R_f 0.20 in 1:1 hexanes−EtOAc; IR (neat) ν_{max} 3231, 1671, 1607, 1513, 1464, 1330, 1113 cm^{-1}; ^{1}H NMR (CDCl₃, 300 MHz) δ 3.97 (6H, s, 2 × OCH₃), 6.12 (1H, brs, OH), 7.15 (2H, s, 2 × ArH), 9.82 (1H, s, CHO); ^{13}C NMR (CDCl₃, 100 MHz) δ 56.41, 106.65, 128.30, 140.81, 147.31, 190.72; HREIMS *m/z* 182.0508 (calcd for C₉H₁₀O₄, 182.0579).

4-(*tert*-Butyldimethylsilyloxy)-3,5-dimethoxybenzaldehyde (7). DI-PEA (4.47 g, 34.6 mmol, 6.02 mL) was added to a stirred solution of 4-hydroxy-3,5-dimethoxybenzaldehyde **6** (4.1 g, 22.47 mmol) and *tert*-butyldimethylsilyl chloride (4.06 g, 26.96 mmol) in anhydrous DMF (100 mL). After the mixture was stirred at room temperature for 18 h, water (100 mL) was added and the reaction mixture extracted with EtOAc (3 × 100 mL). The combined organic phase was washed with water (2 × 50 mL) and dried, and the solvent was removed in vacuo. Separation was achieved by column chromatography, eluting with 1:1 hexanes−EtOAc, to give the title compound in quantitative yield (6.65 g) as an off-white solid: mp 78−79 °C [lit.[28] mp 69−71 °C]; R_f 0.50 in 1:1 EtOAc−hexanes; IR (neat) ν_{max} 2932, 1690, 1503, 1331, 1126 cm^{-1}; ^{1}H NMR (CDCl₃, 300 MHz) δ 0.08 (6H, s, (CH₃)₂Si), 0.93 (9H, s, ^{t}Bu), 3.77 (6H, s, 2 × OCH₃), 7.01 (2H, s, 2 × ArH), 9.72 (1H, s, CHO); ^{13}C NMR(CDCl₃, 100 MHz) δ −4.63, 18.68, 25.58, 55.66, 106.59, 129.28, 140.53, 151.86, 190.88; HRMS APCI$^+$ *m/z* 297.1519 [M + H]$^+$ (calcd for C₁₅H₂₅O₄Si, 297.1522).

4-(*tert*-Butyldimethylsilyloxy)-3,5-dimethoxybenzyl Alcohol (8). A solution of benzaldehyde **7** (6.65 g, 22.47 mmol) in ethanol (30 mL)

was stirred for 10 min at 0 °C. NaBH$_4$ (1.1 g, 29.21 mmol) was added, and the reaction mixture was stirred at 0 °C for 3 h. Solid NaHCO$_3$ was added until effervescing stopped. The solution was filtered and the solvent removed in vacuo. Separation was realized by filtration through a 2 in. silica gel plug, eluting with 1:1 hexanes−EtOAc, to give the alcohol as a colorless solid in 83% (5.54 g) yield: mp 117−118 °C; R_f 0.24 in 7:3 hexanes−EtOAc; IR (neat) ν_{max} 3295, 2932, 2858, 1591, 1511, 1245, 1134, 906 cm^{-1}; ^{1}H NMR (CDCl$_3$, 300 MHz) δ 0.00 (6H, s, (CH$_3$)$_2$Si), 0.89 (9H, s, ^{t}Bu), 1.80 (1H, brs, OH), 3.67 (6H, s, 2 × OCH$_3$), 4.46 (2H, s, CH$_2$OH), 6.42 (2H, s, 2 × ArH); ^{13}C NMR (CDCl$_3$, 100 MHz) δ −4.66, 25.79, 55.73, 65.80, 104.10, 133.37, 151.68; HRMS APCI$^+$ m/z 281.1574 [M + H − H$_2$O]$^+$ (calcd for C$_{15}$H$_{25}$O$_3$Si, 281.1573).

4-(*tert*-Butyldimethylsilyloxy)-3,5-dimethoxybenzyltriphenylphosphonium Bromide (9). To a cooled (0 °C) and stirred solution of alcohol **8** (5.54 g, 18.6 mmol) in anhydrous CH$_2$Cl$_2$ (50 mL) was added a solution of PBr$_3$ (6.04 g, 22.32 mmol, 2.10 mL) in anhydrous CH$_2$Cl$_2$ (25 mL) dropwise at 0 °C. After stirring at 0 °C for 10 min, the reaction mixture was poured onto ice-cold saturated NaHCO$_3$ solution (100 mL). The separated organic phase was washed with water (20 mL) and dried, and the solvent was removed in vacuo to furnish the bromide intermediate. The oily residue was dissolved in toluene (70 mL), and a solution of PPh$_3$ (4.87 g, 18.6 mmol) in toluene (20 mL) was added. The reaction mixture was stirred at room temperature for 10 min. Toluene (∼50 mL) was removed in vacuo, and the reaction mixture was allowed to cool over 24 h. The white precipitate was collected by filtration and recrystallized from ethanol to afford the phosphonium salt in 68% yield (7.89 g) as a colorless solid: mp 246−248 °C; R_f 0.50 in 1:9 CH$_3$OH−CH$_2$Cl$_2$; IR (neat) ν_{max} 3050, 2950, 1511, 1463, 1438, 1338, 1249, 1125 cm^{-1}; ^{1}H NMR (CDCl$_3$, 300 MHz) δ 0.00 (6H, s, (CH$_3$)$_2$Si), 0.89 (9H, s, ^{t}Bu), 3.37 (6H, s, 2 × OCH$_3$), 5.24 (2H, d, J = 13.8 Hz, CH$_2$P), 6.30 (2H, d, J = 2.4 Hz, 2 × ArH), 7.53−7.68 (15H, m, 3 × Ph); ^{31}P NMR (CDCl$_3$, 162 MHz) δ 24.06; HRMS-APCI$^+$ m/z 543.2513 [M − Br]$^+$ (calcd for C$_{33}$H$_{40}$O$_3$PSi, 543.2484).

2,3-Dihydroxy-4-methoxybenzaldehyde (11). Preparation of compound **11** was repeated as originally described[19i] from 2,3,4-trimethoxybenzaldehyde (**10**). Colorless solid, 87% yield: mp 115−116 °C [lit.[19i] mp 115−116 °C]; R_f 0.22 in 1:1 hexanes−EtOAc; IR (neat) ν_{max} 3365, 2944, 1645, 1507, 1453, 1277, 1104, 1025 cm^{-1}; ^{1}H NMR (CDCl$_3$, 300 MHz) δ 3.97 (3H, s, OCH$_3$), 6.62 (1H, d, J = 14.5 Hz, ArH), 7.12 (1H, d, J = 13.5 Hz, ArH), 9.74 (1H, s, CHO); ^{13}C NMR (CDCl$_3$, 100 MHz) δ 56.58, 103.86, 116.32, 126.28, 133.25, 149.29, 153.23, 195.38; HRMS-APCI$^+$ m/z 169.0554 [M + H]$^+$ (calcd for C$_8$H$_9$O$_4$, 169.0500).

2,3-Bis(*tert*-butyldimethylsilyloxy)-4-methoxybenzaldehyde (12). Preparation of compound **12** was repeated as originally described[19c] from benzaldehyde **11**. Additional ^{13}C NMR data are provided here. Colorless solid, 84% yield: mp 75−76 °C [lit.[19c] mp 74.5−76 °C]; R_f 0.76 in 1:1 hexanes−EtOAc; IR (neat) ν_{max} 2932, 2859, 1683, 1585, 1455, 1297, 1099 cm^{-1}; ^{1}H NMR (CDCl$_3$, 300 MHz) δ 0.00 (12H, s, 2 × (CH$_3$)$_2$Si), 0.85 (9H, s, ^{t}Bu), 0.89 (9H, s, ^{t}Bu), 3.70 (3H, s, OCH$_3$), 6.49 (1H, d, J = 14.5 Hz, ArH), 7.36 (1H, d, J = 15.0 Hz, ArH), 10.08 (1H, s, CHO); ^{13}C NMR (CDCl$_3$, 100 MHz) δ −3.92, −3.84, 18.55, 18.74, 26.02, 26.17, 55.17, 105.40, 115.21, 120.75, 121.37, 123.36, 136.80, 150.99, 157.53, 189.26; HRMS APCI$^+$ m/z 397.2234 [M + H]$^+$ (calcd for C$_{20}$H$_{37}$O$_4$Si$_2$, 397.2230).

2′,3′,4-Tris(*tert*-butyldimethylsilyloxy)-3,4′,5-trimethoxy-4-Z- and -E-stilbenes (13, 14). *n*-Butyllithium (13.7 mmol, 5.5 mL, 2.5 M solution in hexane) was added (dropwise) to a stirred and cooled (−20 °C) suspension of triphenylphosphonium bromide **9** (6.2 g, 9.95 mmol) in anhydrous THF (200 mL). The red reaction solution was stirred for 15 min at −15 °C, before addition of benzaldehyde **12** (4.0 g, 10.1 mmol). Stirring was continued at −15 °C for the duration of the experiment. TLC analysis (49:1 hexanes−EtOAc) showed complete conversion to product after 1 h, and the reaction was terminated with the addition of iced water. The reaction mixture was extracted with EtOAc (300 mL), the organic layer was washed with water (100 mL) and dried, and the solvent was removed (in vacuo) to yield a yellow residue. The crude product in ethanol (50 mL) was sonicated to effect solution. The resulting white precipitate was collected and dried to yield a colorless crystalline powder (3.58 g). The ethanol mother liquor was cooled in an ice bath to yield crystals (0.72 g) that had the same R_f value by TLC (95:5 hexanes−EtOAc) as the precipitate. Upon examination by ^{1}H NMR, both precipitate and crystals were found to be the Z-stilbatin 3 derivative **13** and were combined to give 65%

overall yield (4.3 g) of **13**. The remaining mother liquor was concentrated to a yellow oil, which was dissolved in CH$_3$OH and cooled to provide crystals (0.77 g). Examination by ^{1}H NMR showed this product to be a mixture of Z/E-isomers (**13/14**, 0.77 g) in a ratio of 1:3, respectively. Recrystallization of this mixture (0.1 g) from CH$_2$Cl$_2$−CH$_3$OH gave the E-stilbene **14** derivative as needles (0.074 g).

Z-13: mp 110−111 °C, R_f 0.73 in 95:5 hexanes−EtOAc; ^{1}H NMR (CDCl$_3$, 300 MHz) δ 0.08 (6H, s, 2 × (CH$_3$)$_2$Si), 0.102 (6H, s, 2 × (CH$_3$)$_2$Si), 0.171 (6H, s, 2 × (CH$_3$)$_2$Si), 0.980 (18H, s, 2 × (^{t}Bu)), 1.01 (9H, s, ^{t}Bu), 3.59 (6H, s, 2 × OCH$_3$), 3.708 (3H, s, OCH$_3$), 6.29 (1H, d, J = 8.7 Hz, H-5′), 6.34 (1H, d, J = 12.3 Hz, −CH=CH−), 6.56 (2H, s, H-2, H-6), 6.87 (1H, d, J = 8.4 Hz, H-6′); ^{13}C NMR (CDCl$_3$, 125 MHz) δ −4.40, −3.7, −3.0, 18.8, 19.0, 26.0, 26.4, 26.6, 55.2, 55.8, 104.3, 106.3, 122.5, 123.7, 126.5, 128.3, 130.1, 133.6, 137.0, 146.4, 151.3, 151.7; HRMS-APCI m/z 661.3750 [M + H]$^+$ (calcd for C$_{35}$H$_{61}$O$_6$Si$_3$, 661.3776); *anal.* C 63.96%, H 9.24%, calcd for C$_{35}$H$_{60}$O$_6$Si$_3$, C 63.59% H 9.15%.

E-14: mp 118−119 °C, R_f 0.54 in 95:5 hexanes−EtOAc; ^{1}H NMR (CDCl$_3$, 500 MHz) δ 0.11 (6H, s, 2 × (CH$_3$)$_2$Si), 0.13 (6H, s, 2 × (CH$_3$)$_2$Si), 0.14 (6H, s, 2 × (CH$_3$)$_2$Si), 0.99 (9H, s, ^{t}Bu), 1.02 (9H, s, ^{t}Bu), 1.08 (9H, s, ^{t}Bu), 3.79 (3H, s, OCH$_3$), 3.81 (6H, s, 2 × OCH$_3$), 6.54 (1H, d, J = 8.5 Hz, H-5′), 6.68 (2H, s, H-2, H-6), 6.78 (1H, d, J = 16.5 Hz, −CH=CH−), 7.18 (1H, d, J = 8.5 Hz, H-6′), 7.24 (1H, d, J = 16.5 Hz, −CH=CH−); HRMS-APCI$^+$ m/z 661.3782 [M + H]$^+$ (calcd for C$_{35}$H$_{61}$O$_6$Si$_3$, 661.3776); *anal.* C 63.52%, H 9.18%, calcd for C$_{35}$H$_{60}$O$_6$Si$_3$, C 63.59% H 9.15%.

E-Stilstatin 3 (3a). To a cooled (−10 °C) solution of 2′,3′,4-tris(*tert*-butyldimethylsilyloxy)-3,4′,5-trimethoxy-Z-stilstatin 3 (**13**, 6.1 g, 9.23 mmol) in anhydrous THF (30 mL) was added TBAF (11.1 mmol, 11 mL, 1.0 M solution in THF). The reaction mixture was stirred at −10 °C for 50 min. Ice-cold 6 N HCl (2 mL) was added, and the mixture was extracted with EtOAc (4 × 50 mL). The organic phase was dried and the solvent removed in vacuo to afford a brown oil (3.8 g). Purification was realized by column chromatography (eluting with 1:1 hexanes−EtOAc), leading to a pink crystalline powder (1.2 g) that was recrystallized from benzene−chloroform to yield **3a** as colorless crystals: mp 110−111 °C; ^{1}H NMR (CDCl$_3$, 300 MHz) δ 3.88 (3H, s, OCH$_3$), 3.91 (6H, s, 2 × OCH$_3$), 5.39 (1H, s, OH), 5.51 (1H, s, OH), 5.61 (1H, s, OH), 6.47 (d, J = 3 Hz, H-5′), 6.73 (2H, s, H-2, H-6), 7.04−6.98 (2H, m, −CH=CH−, H-6′), 7.15 (1H, d, J = 15.9 Hz, CH=CH); ^{13}C NMR (CDCl$_3$, 100 MHz) δ 56.2, 56.3 (2C), 103.1, 103.2, 117.5, 118.6, 121.4, 128.1, 128.3 (2C), 129.8, 132.3, 134.4, 141.9, 146.1, 147.2; *anal.* C 68.93%, H 6.11%, calcd for C$_{17}$H$_{18}$O$_6$·C$_6$H$_6$, C 69.64%, H 6.05%.

X-ray Crystal Structure of 3a. (a) Data Collection. A small amber crystal block (0.22 mm × 0.19 mm × 0.18 mm) of **3a** grown from a benzene−chloroform solution was mounted on the end of a thin glass fiber using Apiezon type N grease and optically centered. Cell parameter measurements and data collection were performed at ambient temperature (298 ± 1 K) with a Bruker SMART APEX diffractometer using Mo Kα (0.71073 Å) radiation. A sphere of reciprocal space was collected using the Multi-Run scheme available in the Bruker SMART[29] data collection package. Three sets of frames were obtained, with each set using 0.30°/frame steps to cover 182° in ω at fixed φ values of 0°, 120°, and 240°, respectively. Data were integrated and reduced using Bruker SAINT,[29] resulting in 100% coverage of all unique reflections to a resolution of 0.84 Å with an average redundancy of 4.51.

(b) Crystal Data: C$_{17}$H$_{18}$O$_6$·(C$_6$H$_6$)$_{1.5}$, fw = 435.48, monoclinic, $P2_1/c$, a = 6.839(2) Å, b = 16.920(5) Å, c = 19.998(6) Å, β = 94.559(6)°, V = 2306.8(12) Å^3, Z = 4, ρ_c = 1.254 Mg m^{-3}, μ(Mo Kα) = 0.089 mm^{-1}, λ = 0.71073 Å, $F(000)$ = 924.

(c) Structure Solution and Refinement. A total of 18 374 reflections were measured, of which 4068 were independent (R_{int} = 0.0296) and 2864 were considered observed ($I_{obs} > 2\sigma(I)$). Final unit cell parameters were determined by least-squares fit of 6237 reflections covering the resolution range of 8.601 to 0.773 Å. An absorption correction was applied using SADABS[29] on the full data set. Statistical analysis with the XPREP program in SHELXTL[29] indicated that the space group was $P2_1/c$. Routine direct methods structure solution was performed with SHELXTL, which produced all non-hydrogen atom coordinates on the single **3a** molecule in the asymmetric unit. Upon initial refinement with SHELXTL, the remaining solvent in the asymmetric unit became easily discernible in the Fourier difference map. After full isotropic refinement, the thermal parameters for all non-hydrogen atoms

were then allowed to refine anisotropically. Subsequently, hydrogen atoms were added at idealized positions and bond distances with their isotropic thermal parameters fixed at 1.5 times the U_{iso} values of their bonding partners for the methyl and hydroxyl hydrogens and at 1.2 times the U_{iso} values of their bonding partners for all others. The model was then allowed to refine with hydrogens constrained as atoms riding on their bonding partners. This resulted in a final standard residual R_1 value of 0.0528 for observed data and 0.0731 for all data. Goodness of fit on F^2 was 1.022, and the weighted residual on F^2, wR_2, was 0.1432 for observed data and 0.1614 for all data. The final Fourier difference map showed minimal electron density, with the largest difference peak and hole having values of 0.218 electrons $Å^{-3}$ and −0.165 electrons $Å^{-3}$, respectively. Final bond distances and angles were all within expected and acceptable limits for the **3a** molecule. However, the average phenyl C−C distance in the included solvent (1.35 Å) was shorter than typical values (1.39 Å), probably due to the large thermal motion.[30]

2′,3′,4-O-Tri[bis(benzyl)phosphoryl]-3,4′,5-trimethoxy-E-stilbene (15). A solution of *E*-stilstatin 3 (**3a**, 1.5 g, 4.7 mmol) in CCl_3 (7.5 mL) and acetonitrile (8 mL) was cooled to −10 °C. DIPEA (6 mL) and DMAP (0.19 g) were added, and the solution was stirred for several minutes prior to addition of dibenzylphosphite (6.4 g). After 1 h the reaction had not gone to completion (by TLC), and an additional 5 mL of dibenzylphosphite was added to the brown solution. The reaction mixture was stirred at rt for a further 60 min. Next, KH_2PO_4 (0.5 M, 200 mL) was added and the mixture stirred for 10 min before extraction with ethyl acetate (3 × 100 mL). The solution was dried ($MgSO_4$) and the solvent removed in vacuo to yield a brown oil. Column chromatography (99:1 CH_2Cl_2−CH_3OH) provided the desired product as a yellow oil (1.29 g, 24.9% yield): R_f 0.25 (3:7 hexanes−EtOAc); ^1H NMR ($CDCl_3$, 300 MHz) δ 3.66 (6H, s, 2 × OCH_3), 3.79 (3H, s, OCH_3), 5.02 (4H, m, 2 × CH_2Ph), 5.18−5.27 (8H, m, CH_2Ph), 6.64 (2H, s, Ar−H-2,6), 6.80−6.88 (m, 2H, −CH=CH−), 7.12−7.14 (32 H, m, 6 × Ph, 2 × Ar−H); ^{13}C NMR ($CDCl_3$, 125 MHz) δ 55.9 (2C), 56.4, 69.5 (2C), 69.8 (2C), 70.1, 70.2, 103.4 (2C), 109.9, 122.3, 122.6, 127.7−128.9, 134.8, 135.4, 135.5, 135.9, 136.0, 136.3, 151.8, 151.9, 152.0.

Sodium Stilstatin 3: 2′,3′,4-O-Triphosphate Prodrug (3b). To a solution of benzyl phosphate **15** (4.5 g, 4.0 mmol) in anhydrous dichloromethane (150 mL) was added bromotrimethylsilane (3.2 mL, 3.7 g, 24 mmol, 6 equiv) (dropwise), and the reaction mixture stirred at rt for 30 min. The reaction was terminated with the addition of water (100 mL). The phosphoric acid intermediate was not soluble in the organic phase and was immediately converted to the sodium salt by separation and concentration of the aqueous fraction to 30 mL and elution through an ion-exchange column containing Dowex-50W resin (sodium form). The fractions containing the salt were spotted onto TLC plates, and the product-containing fractions were visualized using both UV and I_2 vapor. The pooled fractions were reduced to dryness via freeze-drying for 24 h to yield a cream solid, which was recrystallized from water−ethanol (ice bath at 0 °C) to yield an off-white powder that was collected and dried (2.7 g, 96%): mp 220 °C (chars); ^1H NMR (D_2O, 400 MHz) δ 3.82 (m, 9H, 3 × OCH_3), 6.84 (1 H, d, J = 8.8 Hz, Ar−H), 6.9 (2H, s, Ar−H), 7.0 (1H, d, J = 16.5 Hz, −CH=CH−), 7.4−7.44 (3H, m, Ar−H, −CH=CH−); ^{13}C NMR (D_2O, 100 MHz) δ 56.5, 104.1, 109.0, 120.8, 123.4, 127.7, 130.2, 130.3, 134.6, 134.9, 135.0, 144.0, 152.2, 152.3, 152.4.

Supporting Information Available: X-ray data for *E*-stilstatin 3 (**3a**). This material is available free of charge via the Internet at http://pubs.acs.org.

References and Notes

(1) Part 579 in the Antineoplastic Agents series. For part 578, refer to: Pettit, G. R.; Thornhill, A.; Melody, N.; Knight, J. C. *J. Nat. Prod.* **2009**, *72*, 380−388.

(2) (a) Takaoka, M. J. *J. Fac. Sci. Hokkaido Imp. Univ.* **1940**, *3*, 1−16. (b) Gescher, A. J. *Planta Med.* **2008**, *74*, 1651−1655. (c) Orallo, F. *Curr. Med. Chem.* **2008**, *15*, 1887−1898. (d) Saiko, P.; Szakmary, A.; Jaeger, W.; Szekeres, T. *Mutat. Res.* **2008**, *658*, 68−94. (e) Baur, J. A.; Sinclair, D. A. *Nat. Rev. Drug Discovery* **2006**, *5*, 493−506.

(3) (a) Handler, N.; Brunhofer, G.; Studenik, C.; Leisser, K.; Jaeger, W.; Parth, S.; Erker, T. *Bioorg. Med. Chem.* **2007**, *15*, 6109−6118. (b) Jang, M.; Cai, L.; Udeani, G. O.; Slowing, K. V.; Thomas, C. F.; Beecher, C. W. W.; Fong, H. H. S.; Farnsworth, N. R.; Kinghorn, A. D.; Mehta, R. G.; Moon, R. C.; Pezzuto, J. M. *Science* **1997**, *275*, 218−220.

(4) Tseng, S. H.; Lin, S. M.; Chen, J. C.; Su, Y. H.; Huang, H. Y.; Chen, C. K.; Lin, Y. P.; Chen, Y. *Clin. Cancer Res.* **2004**, *10*, 2190−2202.

(5) Hebbar, V.; Shen, G.; Hu, R.; Kim, B. R.; Chen, C.; Korytko, P. J.; Crowell, J. A.; Levine, B. S.; Kong, A.-N. T. *Life Sci.* **2005**, *76*, 2299−2314.

(6) Garvin, S.; Öllinger, K.; Dabrosin, C. *Cancer Lett.* **2006**, *231*, 113−122.

(7) Wang, Z.; Huang, Y.; Zou, J.; Cao, K.; Xu, Y.; Wu, J. M. *Int. J. Mol. Med.* **2002**, *9*, 77−79.

(8) Naderali, E. K.; Doyle, P. J.; Williams, G. *Clin. Sci. (London)* **2000**, *98*, 537−543.

(9) Cruz, M.; Luksha, L.; Logman, H.; Poston, L.; Agewall, S.; Kublickiene, K. *Am. J. Physiol. Heart Circ. Physiol.* **2006**, *290*, H1969−H1975.

(10) Frankel, E. N.; Waterhouse, A. L.; Kinsella, J. E. *Lancet* **1993**, *341*, 1103−1104.

(11) Wang, Z.; Zou, J.; Cao, K.; Hsieh, T. C.; Huang, Y.; Wu, J. M. *Int. J. Mol. Med.* **2005**, *16*, 533−540.

(12) (a) Bureau, J.; Longpré, F.; Martinoli, M.-G. *J. Neurosci. Res.* **2008**, *86*, 403−410. (b) Chen, G.; Shan, W.; Wu, Y. L.; Ren, L. X.; Dong, I. H.; Ji, Z. Z. *Chem. Pharm. Bull. (Tokyo)* **2005**, *53*, 1587−1590.

(13) Wu, S. L.; Yu, L.; Meng, K. W.; Ma, Z. H.; Pan, C. E. *World J. Gastroenterol.* **2005**, *11*, 4745−4749.

(14) (a) Hung, L. M.; Su, M. J.; Chu, W. K.; Chiao, C. W.; Chan, W. F.; Chen, J. K. *Br. J. Pharmacol.* **2002**, *135*, 1627−1633. (b) Hung, L. M.; Chen, J. K.; Huang, S. S.; Lee, R. S.; Su, M. J. *Cardiovasc. Res.* **2000**, *47*, 549−555.

(15) (a) Wood, J. G.; Rogina, B.; Lavu, S.; Howitz, K.; Helfand, S. L.; Tatar, M.; Sinclair, D. *Nature* **2004**, *430*, 686−689. (b) Howitz, K. T.; Bitterman, K. J.; Cohen, H. Y.; Lamming, D. W.; Lavu, S.; Wood, J. G.; Zipkin, R. E.; Chung, P.; Kisielewski, A.; Zhang, L. L.; Scherer, B.; Sinclair, D. A. *Nature* **2003**, *425*, 191−196.

(16) Walle, T.; Hsieh, F.; DeLegge, M. H.; Oatis, J. E., Jr.; Walle, U. K. *Drug Metab. Dispos.* **2004**, *32*, 1377−1382.

(17) Cardile, V.; Chillemi, R.; Lombardo, L.; Sciuto, S.; Spatafora, C.; Tringali, C. *J. Biosci.* **2007**, *62*, 189−195.

(18) Murias, M.; Jäger, W.; Handler, N.; Erker, T.; Horvath, Z.; Szekeres, T.; Nohl, H.; Gille, L. *Biochem. Pharmacol.* **2005**, *69*, 903−912.

(19) (a) Pettit, G. R.; Cragg, G. M.; Herald, D. L.; Schmidt, J. M.; Lohavanijaya, P. *Can. J. Chem.* **1982**, *60*, 1374−1376. (b) Pettit, G. R.; Singh, S. B.; Cragg, G. M. *J. Org. Chem.* **1985**, *50*, 3404−3406. (c) Pettit, G. R.; Singh, S. B.; Niven, M. L.; Hamel, E.; Schmidt, J. M. *J. Nat. Prod.* **1987**, *50*, 119−131. (d) Pettit, G. R.; Singh, S. B. *Can. J. Chem.* **1987**, *65*, 2390−2396. (e) Pettit, G. R.; Singh, S. B.; Hamel, E.; Lin, C. M.; Alberts, D. S.; Garcia-Kendall, D. *Experientia* **1989**, *45*, 209−211. (f) Pettit, G. R.; Singh, S. B.; Boyd, M. R.; Hamel, E.; Pettit, R. K.; Schmidt, J. M.; Hogan, F. *J. Med. Chem.* **1995**, *38*, 1666−1672. (g) Pettit, G. R.; Rhodes, M. R.; Herald, D. L.; Chaplin, D. J.; Oliva, D. *Anticancer Res.* **1998**, *13*, 981−993. (h) Pettit, G. R.; Rhodes, M. R. *Anti-Cancer Drug Des.* **1998**, *13*, 183−191. (i) Pettit, G. R.; Lippert, J. W., III. *Anti-Cancer Drug Des.* **2000**, *15*, 203−216. (j) Pettit, G. R.; Grealish, M. P.; Jung, M. K.; Hamel, E.; Pettit, R. K.; Chapuis, J.-C.; Schmidt, J. M. *J. Med. Chem.* **2002**, *45*, 2534−2542.

(20) (a) Alloatti, D.; Giannini, G.; Cabri, W.; Lustrati, I.; Marzi, M.; Ciacci, A.; Gallo, G.; Tinti, M. O.; Marcellini, M.; Riccioni, T.; Guglielmi, M. B.; Carminati, P.; Pisano, C. *J. Med. Chem.* **2008**, *51*, 2708−2721. (b) Zou, Y.; Xiao, C.-F.; Zhong, R.-Q.; Wei, W.; Huang, W.-M.; He, S.-J. *J. Chem. Res.* **2008**, 354−356. (c) Pinney, K. G.; Jelinek, C.; Edvardsen, K.; Chaplin, D. J.; Pettit, G. R. In *Anticancer Agents from Natural Products*; Cragg, G. M., Kingston, D. G. I., Newman, D. J., Eds.; Taylor and Francis: Boca Raton, FL, 2005; pp 23−46. (d) Cirla, A.; Mann, J. *Nat. Prod. Rep.* **2003**, *20*, 558−564. (e) Pettit, G. R. In *Anticancer Agents: Frontiers in Cancer Chemotherapy*; Ojima, I., Vite, G. D., Altmann, K.-H., Eds.; American Chemical Society: Washington, DC, 2001; pp 16−42.

(21) Lin, H.-L.; Chiou, S.-H.; Wu, C.-W.; Lin, W.-B.; Chen, L.-H.; Yang, Y.-P.; Tsai, M.-L.; Uen, Y.-H.; Liou, J.-P.; Chi, C.-W. *J. Pharmacol. Exp. Ther.* **2007**, *323*, 365–373.

(22) (a) Zhang, F.; Sun, C.; Wu, J.; He, C.; Ge, X.; Huang, W.; Zou, Y.; Chen, X.; Qi, W.; Zhai, Q. *Pharmcol. Res.* **2008**, *57*, 318–323. (b) Sun, C.; Zhang, F.; Ge, X.; Yan, T.; Chen, X.; Shi, X.; Zhai, Q. *Cell Metabol.* **2007**, *6*, 307–319.

(23) Pettit, G. R.; Rhodes, M. R.; Herald, D. L.; Hamel, E.; Schmidt, J. M.; Pettit, R. K. *J. Med. Chem.* **2005**, *48*, 4087–4099.

(24) Pettit, G. R.; Anderson, C. R.; Herald, D. L.; Jung, M. K.; Lee, D. J.; Hamel, E.; Pettit, R. K. *J. Med. Chem.* **2003**, *46*, 525–531.

(25) Hammond, G. S.; Saltiel, J.; Lamola, A. A.; Turro, N. J.; Bradshaw, J. S.; Cowan, D. O.; Counsell, R. C.; Vogt, V.; Dalton, C. *J. Am. Chem. Soc.* **1964**, *86*, 3197–3217.

(26) Silverberg, L. J.; Dillon, J. L.; Vemishetti, P. *Tetrahedron Lett.* **1996**, *37*, 771–774.

(27) Ren, X.; Chen, X.; Peng, K.; Xie, X.; Xia, Y.; Pan, X. *Tetrahedron: Asymmetry* **2002**, *13*, 1799–1804.

(28) Snider, B. B.; Grabowski, J. F. *Tetrahedron* **2006**, *62*, 5171–5177.

(29) *SMART (Version 5.632), SAINT (Version 6.45a), SHELXTL (Version 6.14), and SADABS (Version 2.10)*; Bruker AXS Inc.: Madison, WI, 2003.

(30) CCDC 736738 (**3a**) contains the supplementary crystallographic data for **3a**. These data can be obtained free of charge from The Cambridge Crystallographic Data Centre via www.ccdc.cam.ac.uk/data_request/cif.